JVI Journals.ASM.org

Early Antigen Presentation of Protective HIV-1 KF11Gag and KK10Gag Epitopes from Incoming Viral Particles Facilitates Rapid Recognition of Infected Cells by Specific CD8$^+$ T Cells

Henrik N. Kløverpris,[a] Rebecca P. Payne,[a] Jonah B. Sacha,[b] Jane T. Rasaiyaah,[c] Fabian Chen,[d] Masafumi Takiguchi,[e] Otto O. Yang,[f] Greg J. Towers,[c] Philip Goulder,[a] Julia G. Prado[g]

Department of Paediatrics, University of Oxford, United Kingdom[a]; Vaccine & Gene Therapy Institute, Oregon National Primate Research Center, Oregon Health & Science University, Portland, Oregon, USA[b]; Medical Research Council Centre for Medical Molecular Virology, Division of Infection and Immunity, University College London, London, United Kingdom[c]; Department of Sexual Health, Royal Berkshire Hospital, Reading, United Kingdom[d]; Centre for AIDS Research, Kumamoto University, Kumamoto, Japan[e]; Departments of Medicine and Microbiology, Immunology, and Molecular Genetics, David Geffen School of Medicine, University of California, Los Angeles, California, USA[f]; AIDS Research Institute IrsiCaixa, Hospital Universitari Germans Trias i Pujol, Badalona, Barcelona, Spain[g]

CD8$^+$ T cells are major players in antiviral immunity against human immunodeficiency virus type 1 (HIV-1) through recognition of viral epitopes presented on the surface of infected cells. However, the early events involving HIV-1 epitope presentation to CD8$^+$ T cells remain poorly understood but are nonetheless crucial for the rapid clearance of virus-infected cells. Here, we comprehensively studied the kinetics of antigen presentation of two protective epitopes, KF11Gag and KK10Gag, restricted by HLA alleles B*57:01 and B*27:05, respectively, and compared these to KY9Pol and VL9Vpr epitopes in a single cycle of HIV-1 replication. We consistently demonstrate differences in epitope presentation kinetics, with very early presentation, within 3 h postinfection, for the protective KF11Gag, KK10Gag epitopes, and KY9Pol but only late presentation for VL9Vpr. We show that this early presentation relies on the antigen being presented from incoming viral particles and is correlated with rapid CD8$^+$ T cell activation and clearance of virus-infected cells. Additionally, our data indicate a dose-response dependency between the levels of CD8$^+$ T cell activation and the amount of virus inoculum. These data reflect a proof of principle emphasizing the importance of identifying early-presented viral epitopes for rapid elimination of HIV-1-infected cells.

CD8$^+$ T cells are an important component of the adaptive immune system with a crucial function in controlling intracellular pathogens. CD8$^+$ T cells recognize pathogen-derived peptides in the context of HLA class I molecules on the surface of infected cells to mediate their killing. In the last decade, much effort has focused on the design of vaccines that aim to control intracellular pathogens such as human immunodeficiency virus type 1 (HIV-1) through the induction of potent CD8$^+$ T cell responses (1, 2). The attempt to design CD8$^+$ T cell-mediated vaccines against HIV-1 is based on strong evidence supporting the role of CD8$^+$ T cell responses in the control of virus replication (3). Various studies suggest that host genetic traits, such as the expression of certain HLA class I molecules, are related to HIV-1 control (4–6). Additionally, HIV-1 Gag targeting (7), virus immune escape facilitating virus attenuation (8, 9), and the quality of the CD8$^+$ T cell responses have been independently linked to HIV-1 immune control (10–13).

However, a common limitation for the characterization of CD8$^+$ T cell responses is the use of artificial exogenous peptides in functional assays, such as enzyme-linked immunospot assay (ELISpot), to determine the breadth and magnitude of CD8$^+$ T cell responses. Recognition of exogenous peptides by CD8$^+$ T cells in these assays does not necessarily reflect true antiviral activity through recognition of HIV-1-infected cells displaying endogenously processed peptides (14). Two reasons for this are that the antigen-processing machinery within infected cells is bypassed and that peptides in such assays are used at nonphysiological concentrations. Alternative approaches, such as those involving the use of HIV-1-infected cells (15–17), provide additional information related to direct CD8$^+$ T cell-mediated antiviral activity and the kinetics of epitope presentation.

In recent years, various studies have demonstrated the importance of epitope presentation timing for subsequent clearance of virus-infected cells. However, these studies were mainly carried out in the simian immunodeficiency virus (SIV) model (18–21) and the majority of studies on HIV-1 have not focused on a single cycle of virus replication (22, 23). Consequently, despite the large number of HIV-1 epitopes described to date, very little is known about the early events of epitope presentation and their contribution to rapid clearance of virus-infected cells. We recently developed an *in vitro* model system to examine anti-HIV-1 CD8$^+$ T cell activity mediated by presentation of various viral epitopes (24). In the present work, we used this experimental approach to further assess, in various cell types, the kinetics and mechanisms underlying early antigen presentation. For this purpose, we focused on two important immunodominant HIV-1 epitopes, KF11Gag and KK10Gag, restricted by HLA-B*57:01 and HLA-B*27:05, respectively, known to be involved in superior *in vivo* viral control (7, 8, 25–28). We compared these with two epitopes, KY9Pol and

Received 12 August 2012 **Accepted** 11 December 2012
Published ahead of print 19 December 2012
Address correspondence to Julia G. Prado, jgarciaprado@irsicaixa.es.

doi:10.1128/JVI.02131-12

TABLE 1 Clinical data and *ex vivo* ELISpot responses for study subjects

Subject ID	HLA genotype	Viral load (RNA copies/ml)	$CD4^+$ T count (cells/ml)	Time postinfection (mo)	Overlapping peptide response[a]	Magnitude[b] ($SFU/10^6$ PBMCs)	Protein	Optimal epitope tested	HLA restriction allele	Magnitude ($SFU/10^6$ PBMCs)	Protein
R035	A*02:01/24:02 B*27:05/44:02 Cw*02:02/05:01	13,470	900	16	PVGEIYKRWIILGLNKIV	460	Gag	VRHFPRIWL	B*27:05	165	Vpr
					SILDIRQGPKEPFRDYV	60	Gag				
					KTVRLIKFLYQSNPPPS	170	Rev				
					QARRNRRRRWRERQRQIR	310	Rev				
					SLQYLALAALITPKKIK	140	Vif				
					IKPPLPSVTKLTEDRWNK	110	Vif				
R039	A*01:01/31:01 B*27:05/57:01 Cw*02:02/06:02	204	650	9	WVKVVEEKAFSPEVIPMF	535	Gag	KAFSPEVIPMF	B*57:01	520	Gag
					PVGEIYKRWIILGLNKIV	615	Gag	KRWIILGLNK	B*27:05	320	Gag
					LWVYHTQGYFPDWQNY	235	Nef	KRKGGIGGY	B*27:05	1,180	Pol
					AVFIHNFKRKGGIGGYSA	615	Pol				

[a] The characterized epitopes are underlined (data from the Los Alamos Immunology database, www.hiv.lanl.gov).
[b] First ELISpot data available. SFU, spot-forming units.

VL9Vpr, restricted by HLA-B*27:05 and generated pure HIV-1-specific $CD8^+$ T cell lines to define the kinetics of epitope presentation. In addition, we refined our previous model to demonstrate the role of incoming viral particles to deliver early epitope presentation and killing of virus-infected cells and to underline once again, the importance of using virus-infected cells for *in vitro* models in order to characterize activity of HIV-1-specific $CD8^+$ T cells.

MATERIALS AND METHODS

Study subjects. Patient material for *in vitro* assays was derived from 2 treatment-naïve individuals with chronic HIV-1 infection. Patients were HLA typed as described in reference 7 and recruited from a local cohort of treatment-naïve HIV-1-infected individuals in England. Clinical data and HIV $CD8^+$-specific responses measured by ELISpot are included in Table 1. Informed consent was obtained from the participating individuals. The institutional review board at the University of Oxford approved the study.

Cell lines. To assess epitope presentation of HLA-B*27:05-restricted epitopes, the HIV-1-permissive U937 cell line transfected with the HLA-B*27:05 gene was used as target cells (24). The HLA-B*57:01-restricted KF11Gag epitope was assessed using the H9 T cell clone transduced with HLA-B*57:01. HLA-mismatched $CD4^+$ cell lines were either U937, H9, or the human lymphoblastoid NK target cell line .221, expressing $CD4^+$ and either HLA-B*1503 or HLA-B*1510 (29). All cells were cultured in RPMI medium with 10% fetal calf serum (FCS) (HyClone), L-glutamine, penicillin, and streptomycin (R10). Selection antibiotic geneticin or kanamycin was added to R10 culture medium for U937 and .221 cell lines, respectively. Primary $CD4^+$ T cells were freshly isolated human peripheral blood mononuclear cells (PBMCs), which were subsequently activated using phytohemagglutinin (PHA) (10 μg/ml) and staphylococcus enterotoxin B (1 μg/ml) (SEB) for 4 days, cultured in R10. Specific $CD8^+$ T cell lines were generated as previously described (24).

Virus and virus-like particle (VLP) production. Viral stocks were produced by cotransfection in MT4 cells of p83-2 and p83-10eGFP plasmids derived from NL4-3 plasmid as previously described (30, 31). Virus was harvested and stored at −80°C, and the 50% tissue culture infective dose ($TCID_{50}$) for each viral stock was determined in MT4 cells using the Reed and Muench method.

HIV-1 GFP VLPs (HIV-VLPs) pseudotyped with the vesicular stomatitis virus G (VSV-G) protein envelope were produced by transfecting the HIV-1 packaging plasmid pCMVΔR8.2 (which encodes all HIV-1 proteins except gp160 envelope protein) (32), the green fluorescent protein (GFP)-encoding vector genome pCSGW (which does not encode any HIV-1 proteins) (33), and the VSV-G-encoding plasmid pMDG (34) into 293T cells using Fugene-6 (Roche), as previously described (35). The supernatant contained virions consisting of all the normal components of HIV-1 particles including Gag, Pol, and Vpr with the natural HIV-1 envelope protein replaced with the VSV-G envelope protein. Because the packaged genome inside the VLP does not encode HIV-1 proteins, then VLP-infected cells express only GFP and cannot synthesize any viral proteins. Therefore, all viral proteins inside the infected cell are derived from incoming VLPs and not from *de novo* protein transcription. Supernatant from transfected 293T cells was purified by ultracentrifugation through a 20% sucrose cushion. The HIV-VLP dose was measured by reverse transcriptase (RT) enzyme-linked immunosorbent assay (ELISA) (Roche) according to the manufacturer's instructions. The functional titer of HIV-VLP was determined on GHOST cells, where 1 ng RT is equivalent to 2×10^7 infectious units (35). In the experiments described, a multiplicity of infection (MOI) of 1 based on the GHOST titer gives an MOI of around 0.2 on B cell line (BCL) cells and an MOI of 1 on U937 cells due to differences in cell permissiveness to infection (data not shown). Sequences of Gag, Pol, and Vpr epitopes are identical in plasmids pCMVΔR8.2 and p83-2, used to generate VLP and HIV, respectively. Both plasmids are derived from NL4.3 GenBank accession code M19921 and carry the optimal epitope sequence defined in the Los Alamos Immunology database and used to grow the specific $CD8^+$ T cell lines (Table 2).

Epitope presentation assay. Epitope presentation and killing of virus-infected cells were assessed by adapting a previously described method (36) to the human system. $CD4^+$ target cells were synchronously infected with HIV-1 using an MOI of 1 as described in reference 24, and an HIV reverse transcriptase inhibitor (AZT; Invitrogen) was used at a 5 μM final concentration, as previously described (19), throughout the assay when indicated. In addition, we used HIV-1 virus-like particles pseudotyped with the G protein of vesicular stomatitis virus. Target cells were infected with 1 ng of RT of HIV-VLP per million cells for 2 h before incubation and coculture at an effector-to-target ratio of 1:2 in the presence of anti CD107a (BD). Therefore, for HIV-VLP assays, we were not able to harvest cells at the first time point before 2 h postinfection. For all experiments, at each time point, one-fifth of the sample was recovered and incubated in the presence of brefeldin A and GolgiStop for 3 h and then stored. All samples were stained for the following markers: CD8 (Alexa Fluor 750 from eBioscience; or V-450 from BD-Pharmingen), CD4 (Qdot 605 from Invitrogen or APC from BD-Pharmingen), live/dead marker (Invitrogen), gamma interferon (IFN-γ) (BD-Pharmingen), MIP1β (R&D), and anti-HIV-1 p24 Gag (KI-57 from Beckmann Coulter). Peptide-pulsed (25 μg/ml) $CD4^+$ target cells were included as controls. All samples were acquired on an LSR II flow cytometer from BD. $CD8^+$ effector cells were gated on forward side scatter, and live cells, CD4-negative cells, and $CD8^+$ cells were gated for expression of effector markers, IFN-γ, CD107a, and MIP1β. Activation of specific $CD8^+$ T cells was calculated as the percentage of the maximum level detected in the CD107a/MIP1β gate of any of the $CD8^+$ T cell lines used (100%) within the same experiment. Target cells were gated on forward side

TABLE 2 HIV-specific $CD8^+$ T cell lines and viral vectors used in the study

Subject ID	HLA restriction allele	Epitope	Protein	Amino acid position in HXB2	Viral vector	HIV clade B sequence	% $CD8^+$ T cell line specificity[b]
R039	HLA-B*57:01	KF11	Gag	162–172	Seq database[a]	KAFSPEVIPMF	98.4
					NL4-3	----------	
					pCMVΔR8.2	----------	
R039	HLA-B*27:05	KK10	Gag	263–272	Seq database	KRWIILGLNK	99.6
					NL4-3	----------	
					pCMVΔR8.2	----------	
R039	HLA-B*27:05	KY9	Pol	186–194	Seq database	KRKGGIGGY	98.4
					NL4-3	---------	
					pCMVΔR8.2	---------	
R035	HLA-B*27:05	VL9	Vpr	31–39	Seq database	VRHFPRIWL	99.4
					NL4-3	---------	
					pCMVΔR8.2	---------	

[a] Seq database, Los Alamos Immunology database (www.hiv.lanl.gov).
[b] Tetramer-positive $CD3^+CD8^+$ gated T cells.

scatter, live cells and analyzed in a $CD4^+$ versus p24-PE or $CD4^+$ versus GFP-fluorescein isothiocyanate (FITC) double dot plot. All samples were analyzed using FlowJo software V8.8.6 (Tree Star, Inc.). Killing efficiencies were calculated as follows: (% $p24^+$ or GFP^+ $CD4^+$ cocultured with specific $CD8^+$ T cells)/(% $p24^+$ or GFP^+ $CD4^+$ without any $CD8^+$ T cells) $\times 100$.

TcR affinity and polyfunctionality. The functional avidity and polyfunctionality of epitope-specific $CD8^+$ T cells were investigated by intracellular cytokine staining (ICS) assay using a multiparameter antibody panel. Log_{10} serial peptide titrations pulsed on an HLA-matched B cell line were cocultured for 3 h with HIV-1-specific $CD8^+$ T cell lines in the presence of brefeldin A and GolgiStop followed by staining of CD8 (BD-Pharmingen), CD3 (BD-Pharmingen), Live/Dead marker (Invitrogen), CD107a (BD-Pharmingen), MIP1β (R&D), or IFN-γ (BD). T cell receptor (TcR) avidity was calculated for percent IFN-γ expression gated on $CD8^+$ T cells that resulted in 50% maximum (50% inhibitory concentration [IC_{50}]) using GraphPad Prism V5.0a. Polyfunctional assessments of simultaneous expression of CD107a, MIP1β, and IFN-γ for comparison of effector marker profiles were analyzed using Pestle V1.6.2 and Spice V4.3. All samples were acquired on an LSR II flow cytometer and analyzed using FlowJo V8.8.6.

RESULTS

KF11Gag, KK10Gag, and KY9Pol HIV-1-derived $CD8^+$ T cell epitopes are presented early after infection of $CD4^+$ T cells. To investigate the kinetics of epitope processing and presentation in $CD4^+$ T cells following HIV-1 infection, we first focused on the $CD8^+$ T cell epitope restricted by HLA-B*57:01, KF11Gag, which is associated *in vivo* with control of HIV-1 (7, 8, 25). Pure $CD8^+$ T cell lines to >95% specificity for KF11Gag were generated (Table 1). To ensure synchronous infection of target cells, we adopted the previously described "magnetofection" method (36). Subsequently, we cocultured KF11Gag-specific $CD8^+$ T cells in two different HIV-1-infected cell types expressing HLA-B*57:01, H9 cells transduced with HLA-B*57:01, and primary $CD4^+$ T cells. In order to determine the background levels of potential nonspecific activation of the $CD8^+$ T cell lines tested (independent of viral infection and epitope presentation), we infected HLA-mismatched cells and cocultured them with each of the $CD8^+$ T cells used in the experiments. No nonspecific activation was observed in any of the background controls (Fig. 1C and D). Additionally, similar levels of HIV-1-infected cells were measured at the beginning of the experiment for the HLA-matched and -mismatched $CD4^+$ cell lines. Therefore, differences in activation between those cell types could not be attributed to variations in the amount of incoming viral particles available for antigen processing and presentation.

For all experiments, the readout of epitope presentation was dual staining of CD107a and MIP1β in $CD8^+$ T cell lines, since these markers have been previously shown to be crucial for $CD8^+$ T cell antiviral activity (7) and in our hands are the most sensitive markers for activation of HIV-specific $CD8^+$ T cell lines in these assays (Fig. 1A).

We first showed that KF11Gag-specific $CD8^+$ T cells are activated by HIV-infected HLA-matched targets within 3 h of infection (Fig. 1A). We controlled for the expression of HLA-B*57:01 and the KF11Gag specificity by peptide pulsing matched $CD4^+$ T cells (Fig. 1B). We observed a two-phase kinetics of epitope presentation in both H9 and primary $CD4^+$ T cells for KF11Gag with early presentation at 3 to 6 h followed by a boost of activation at 18 h postinfection (Fig. 1C).

To compare the kinetics of antigen presentation of KF11 Gag with those of other HIV-1-specific epitopes associated with control of viremia, we generated pure $CD8^+$ T cell lines for the HLA-B*27:05-restricted KK10Gag and included two additional epitopes, KY9Pol and VL9Vpr, also restricted by HLA-B*27:05 for comparison (Table 2). Using the same experimental approach, we observed a similar two-phase kinetics of early epitope presentation for the KK10Gag and KY9Pol epitopes (3 to 6 h), with a second wave of activation between 18 and 24 h (Fig. 1D). In contrast, the VL9Vpr epitope showed a marked difference in presentation kinetics, with partial $CD8^+$ T cell activation only at later time points. Thus, these data demonstrate comparable kinetics of early presentation for known KF11Gag and KK10Gag protective epitopes together with KY9Pol, in contrast to the VL9Vpr epitope, which is recognized only at later time points.

Early kinetics of epitope presentation rely on antigen processing in the absence of virus replication. The early presentation kinetics for KF11Gag, KK10Gag, and KY9Pol epitopes suggest that activation of specific $CD8^+$ T cells do not depend on *de novo* synthesis of viral protein to access the class I processing pathway. In order to establish unequivocally the contribution from incoming HIV-1 particles to the kinetics of early epitope presentation, we developed a single-cycle infection system based on pseu-

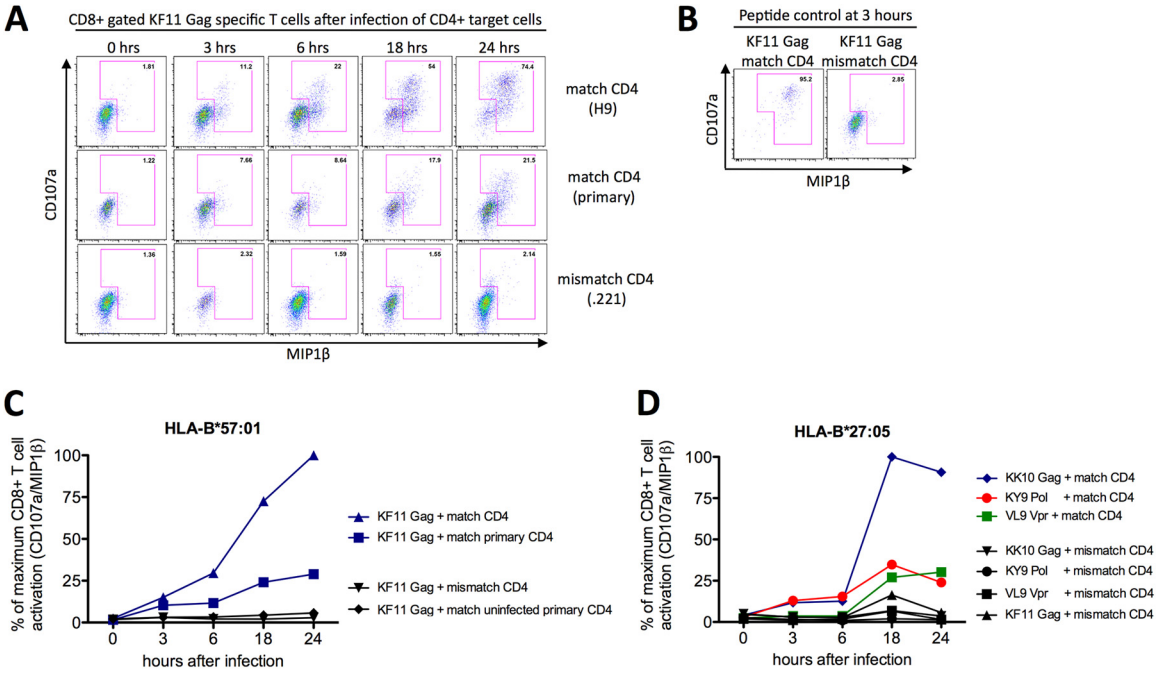

FIG 1 KF11Gag, KK10Gag, and KY9Pol epitopes are presented early after wild-type (WT) HIV-1 infection. Fluorescence-activated cell sorting (FACS) dot plots showing CD107a/MIP1β-expressing HLA-B*57:01-restricted KF11Gag-specific $CD8^+$-gated T cells after coculture at 0, 3, 6, 18, and 24 h with HLA-matched and -mismatched WT HIV-1-infected $CD4^+$ T cells (A) or with KF11 peptide-pulsed HLA-matched or -mismatched $CD4^+$ T cells (B) and plotted on a graph for 5 time points throughout 24 h after infection (C). Activation of KK10Gag-, KY9Pol-, and VL9Vpr-specific $CD8^+$ T cells restricted by HLA-B*27:05 after coculture with HIV-1-infected HLA-matched U937 $CD4^+$ cells or mismatched H9 $CD4^+$ T cells at 0, 3, 6, 18, and 24 h postinfection. (D) Results from one experiment representative of three independent experiments are shown.

dotyped HIV-1 VLPs encoding GFP. The VLPs encode GFP rather than viral proteins, and therefore infected cells become green but cannot express any viral proteins. In this way, we can monitor virus infection by the expression of GFP in the target cells (Fig. 2). Thus, we used HIV-VLP to infect a B cell line expressing both HLA-B*27:05 and HLA-B*57:01. We observed early presentation and similar kinetics for both KF11Gag- and KK10Gag-specific $CD8^+$ T cell activation in the absence of HIV-1 protein transcription (Fig. 3A and B). In addition, the KY9Pol-specific $CD8^+$ T cells were also activated within the same time, although no increase in activation was detected over time (Fig. 3B). In contrast,

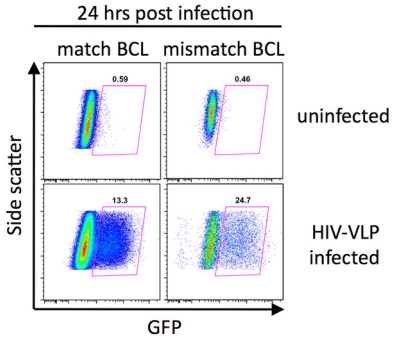

FIG 2 B cell line infection with HIV-VLP expressing GFP. B cell lines expressing both HLA-B*27:05 and B*57:01 and an HLA-mismatched B cell line were infected with 1 ng RT of VSV-G-pseudotyped HIV-VLP expressing GFP. Infection was measured by flow cytometry 24 h postinfection. GFP expression was controlled by determining the number of uninfected cells.

the VL9Vpr-specific $CD8^+$ T cells did not see any cognate antigen presented from the HIV-VLP infection and sustained dependency on the *de novo* synthesis of proteins for VL9Vpr epitope presentation.

Once we established the role of incoming viral particles in early epitope presentation for both KF11Gag and KK10Gag in BCL, we confirmed our results using HIV-VLP in an alternative target cell line (U937 expressing CD4) for the HLA-B*27:05-restricted epitopes. In agreement with previous data, we found a similar hierarchy of antigen presentation for all epitopes tested (Fig. 3C and D). Remarkably, both the KK10Gag- and KY9Pol-specific $CD8^+$ T cell lines reached a peak of activation (5 to 8 h in the case of KK10 Gag and 8 to 20 h for KY9Pol), which additionally supports that, in the absence of virus replication, activation occurs only when cognate antigen is available for the $CD8^+$ T cells as confirmed by the results for VL9Vpr epitope. To further validate our results, we conducted a similar experiment using fully competent HIV-1 in U937 and primary $CD4^+$ T cells expressing HLA-B*27:05 as target cells in the presence of an HIV-1 reverse transcriptase inhibitor (AZT), which results in the suppression of HIV-1 protein transcription. We obtained similar findings with KK10Gag and KY9Pol presentation but no VL9Vpr epitope presentation at 24 h postinfection (Fig. 4A and B). Decreased antigen presentation was unrelated to potential cellular toxicity mediated by AZT treatment (Fig. 4C and D). Of note, although the HIV-1 epitope hierarchy was maintained between cell lines, we observed a divergence in the dynamics of antigen presentation

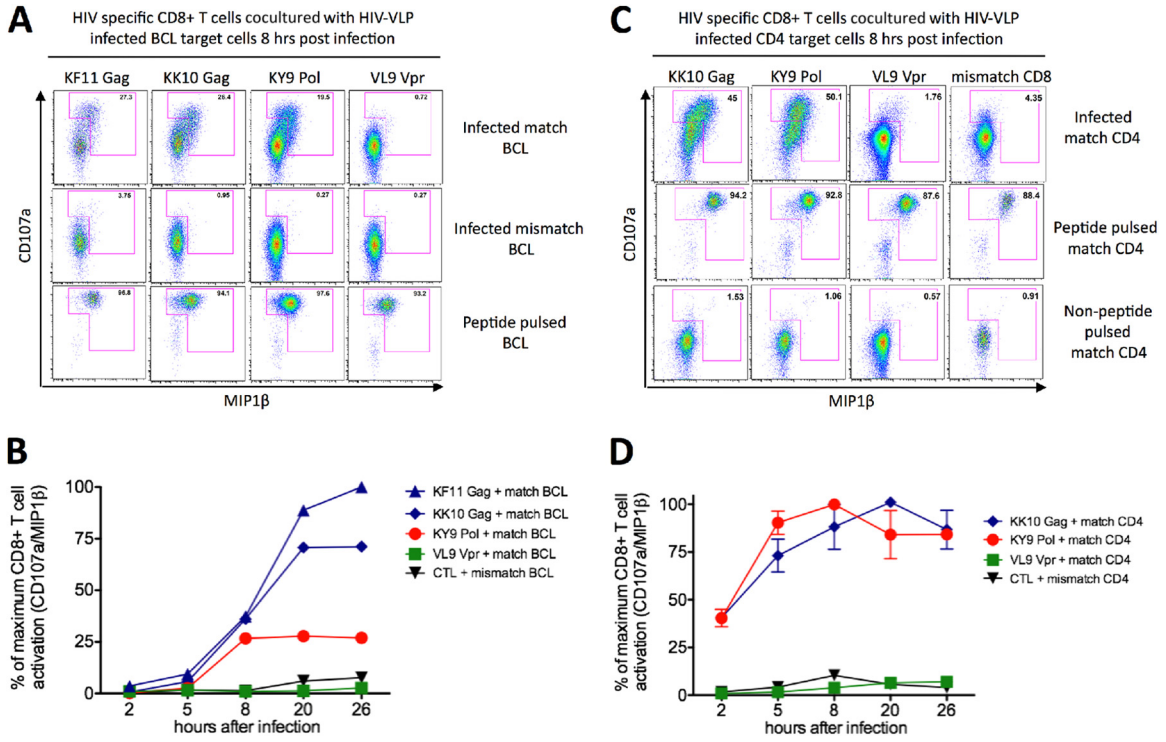

FIG 3 KF11Gag, KK10Gag, and KY9Pol epitopes are processed from the incoming viral particles. Fluorescence-activated cell sorting (FACS) dot plots showing CD107a/MIP1β-expressing KF11Gag-, KK10Gag-, KY9Pol-, and VL9Vpr-specific $CD8^+$-gated T cells after coculture at 2, 5, 8, 20, and 26 h with HLA-matched and -mismatched B cell lines infected with HIV-VLP or peptide pulsed (A) and plotted on a graph for 5 time points throughout 26 h (B). (C and D) Results of assays as described for panels A and B, respectively, but using HLA-B*27:05 $CD4^+$-expressing infected U937 cells. Graphs present mean values and standard errors of the means from triplicates.

with the use of either the BCL or the U937 cells. Thus, the faster kinetics found for the U937 cells could be related to the monocytic origin of the cells and their specialization as antigen-presenting cells.

The use of the HIV-VLP system provides clear evidence that the KF11Gag, KK10Gag, and KY9Pol epitope presentation kinetics depends on preformed protein derived from incoming viral particles in the absence of virus replication, whereas VL9Vpr epitope presentation appears to be entirely dependent on the *de novo* synthesis of protein.

Early presentation of HIV-1 epitopes is associated with early killing of virus-infected cells but is independent of TcR affinity. The early activation of KK10Gag- and KY9Pol-specific $CD8^+$ T cells is related to early epitope presentation, but whether or not differences in $CD8^+$ T cell activation over time translate directly into differences in functional killing of HIV-1-infected cells has not been clearly established. Therefore, we next investigated the ability of KK10Gag-, KY9Pol-, and VL9Vpr-specific $CD8^+$ T cells to eliminate virus-infected cells by measuring the reduction of $p24^+/CD4^+$ cells, using the same HIV-VLP experimental model. We observed a rapid elimination (>50%) of $p24^+/CD4^+$ cells at 5 h and almost complete elimination (>85%) at 20 h postinfection for KK10Gag- and KY9Pol-specific $CD8^+$ T cells (Fig. 5A and B). In contrast, the VL9Vpr-specific $CD8^+$ T cells did not exhibit any killing activity, consistent with the lack of $CD8^+$ T cell activation. We confirmed these observations by measuring the frequency of GFP^+ cells within HIV-VLP-infected cells (Fig. 5C and D). By simultaneous assaying of $CD8^+$ T cell activity and clearance of virus-infected cells, we demonstrate a direct causality between early activation of KK10Gag- and KY9Pol-specific $CD8^+$ T cells and early elimination of virus-infected cells (Fig. 5E). Nevertheless, differences in activation and killing may be attributed to differences in TcR affinity between $CD8^+$ T cells. In order to rule out this hypothesis, we tested TcR affinities after coculture of $CD8^+$ T cells with peptide-pulsed BCLs (Fig. 6) and observed only small differences in 50% effective concentrations (EC_{50}s) between KF11Gag-, KK10Gag-, KY9Pol-, and VL9Vpr-specific $CD8^+$ T cells (log molar EC_{50}, −7.6, −6.6, −7.1, and −7.3, respectively). Importantly, EC_{50}s do not explain the differential hierarchy of killing shown above. Moreover, we also compared KF11Gag-, KK10Gag-, KY9Pol-, and VL9Vpr-specific $CD8^+$ T cell lines for granzyme B expression and the direct killing activity against peptide-pulsed target B cell lines and found no differences (data not shown). These data suggest no intrinsic functional differences in response to the HIV-1 antigens between VL9Vpr and the remaining $CD8^+$ T cell specificities studied here. Taken together, these data demonstrate that epitope presentation timing contributes to early $CD8^+$ T cell activation and killing of virus-infected cells.

Total HIV-1-specific $CD8^+$ T cell activation and functionality depend on the amount of antigen presented on virus-infected cells. The discrepancies found in the levels of $CD8^+$ T cell activation between various HIV-1 epitopes suggest that activation is dependent on the amount of epitope presented on the surface of infected cells. Additionally, cytokine activation

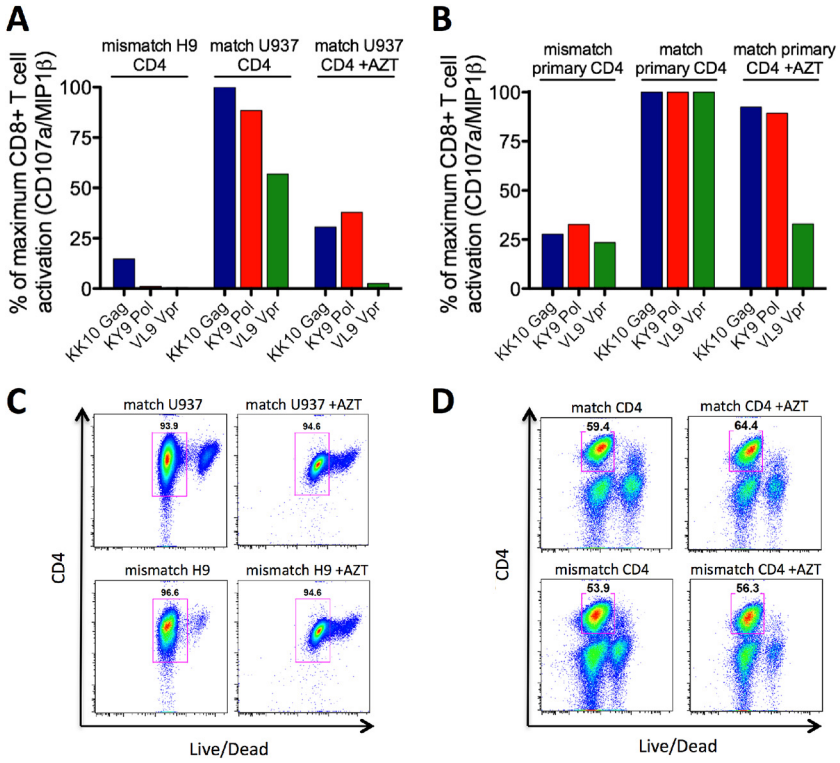

FIG 4 KK10Gag and KY9Pol epitopes are presented in the absence of *de novo* HIV-1 protein synthesis. Percentage of maximum CD107a/Mip1β expression of KK10Gag-, KY9Pol-, and VL9Vpr-specific $CD8^+$ T cells restricted by HLA-B*27:05 after coculture with HIV-1-infected cells in the presence or in the absence of reverse transcriptase inhibition (5 μM AZT). (A) HLA-matched U937 $CD4^+$ cells and mismatched H9 $CD4^+$ T cells; (B) HLA-matched primary infected $CD4^+$ T cells and mismatched primary $CD4^+$ T cells. (C and D) Viability of U937 cells and primary $CD4^+$ T cells with or without AZT treatment at 24 h postinfection.

profiles of $CD8^+$ T cells through HIV-1-infected cells may differ from the profiles obtained in exogenous peptide-loaded experiments. To test the relationship between the levels of antigen presented and the levels of $CD8^+$ T cell activation, we infected the U937 $CD4^+$ cells with HIV-VLP at MOI of 1 and 0.1 and measured the subsequent $CD8^+$ T cell activation in each case. A 10-fold decrease in the amount of virus inoculum resulted in a 2- to 3-fold decrease in the percentage of activated $CD8^+$ T cells (Fig. 7A and B). These data suggest a dose-response dependency between the amount of virus inoculum and the level of $CD8^+$ T cell activation. Throughout the study, we have consistently observed a reduction in activation levels of $CD8^+$ T cells in recognition of virus-infected cells compared to exogenous loaded peptides (20% versus 90%). Therefore, we compared the differences between $CD8^+$ T cell activation stimulated by direct exogenous peptide loading and that stimulated by intracellular processed epitopes after HIV-VLP infection (Fig. 7C). It is clear that exogenous-peptide-pulsed BCLs result in a higher magnitude of total $CD8^+$ T cell activation and a more polyfunctional profile of cytokine secretion for all epitopes tested compared to intracellular processed epitopes (median, 90% versus 24%; $P = 0.03$; data not shown). We can estimate that the use of peptide concentrations in the range of 10^{-6} M in conventional *in vitro* stimulation assays (38, 39) may be 10^3 to 10^5 times higher than the actual amount of intracellular presented epitopes within infected cells based on the levels of $CD8^+$ T cell activation (40). These data suggest that most *in vitro* peptide pulsing studies use nonphysiological concentrations of artificial peptides, which may mask differences between the total activation and polyfunctionality of $CD8^+$ T cells and those of virus-infected cells.

DISCUSSION

This study characterizes the properties in terms of the timing of epitope presentation of two HLA class I-restricted epitopes, KF11Gag and KK10Gag, which are known to play a protective role in HIV-1 immune control (7–9, 25, 26, 28). Our data reveal early antigen presentation within 3 to 6 h after HIV-1 infection, well before virus integration and the *de novo* synthesis of viral proteins (41) for protective KF11Gag and KK10Gag epitopes. The early kinetics also applied to a dominantly targeted KY9Pol epitope (24) but was in contrast to the VL9Vpr epitope, which was presented only at the very late stage of the viral replication cycle.

Consistently, our experiments demonstrate two-phase kinetics of epitope presentation in both primary and immortalized cell lines. We observe a first wave of $CD8^+$ T cell activation at 3 to 6 h after infection followed by a boost of activation at 18 to 24 h. Based on our results, early $CD8^+$ T cell activation for KF11Gag, KK10Gag, and KY9Pol epitopes is related to antigen presentation derived from incoming viral particles in the absence of virus replication as demonstrated by the use of HIV-VLP and supported by previous studies (42–44). Meanwhile, the second wave of epitope presentation is presumably related to viral protein synthesis and

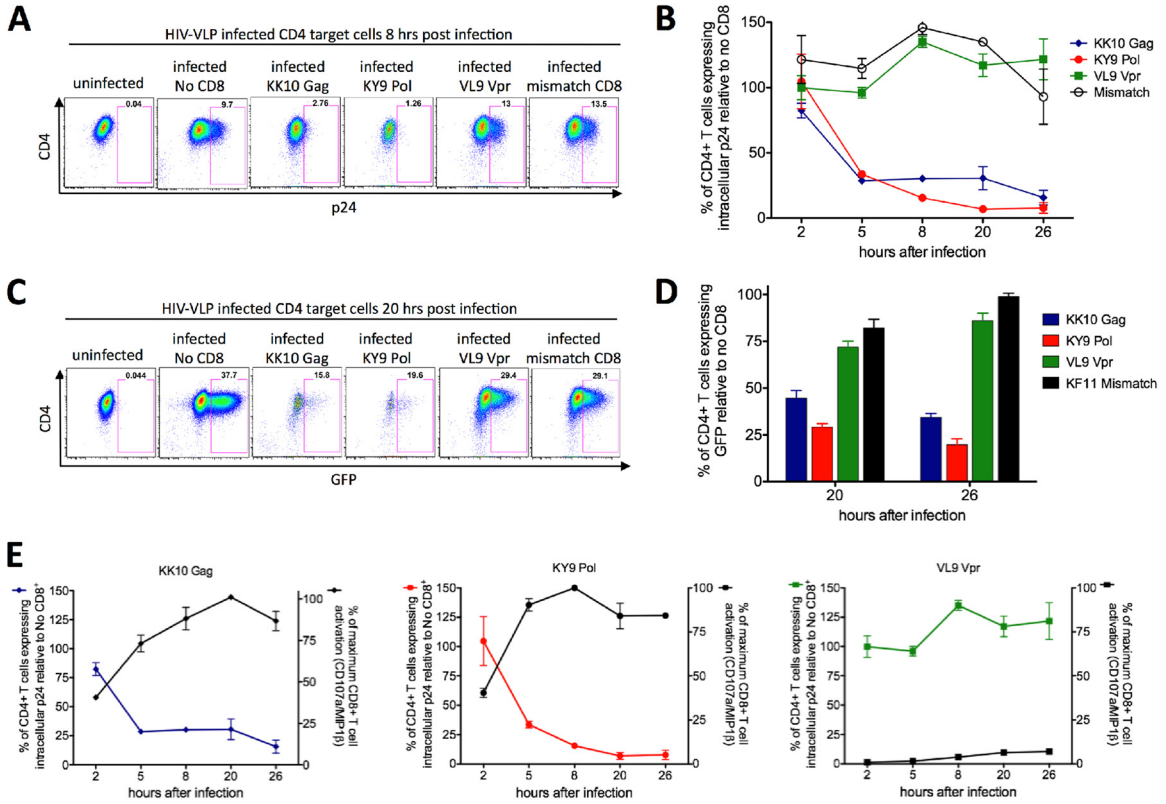

FIG 5 KK10Gag- and KY9Pol-specific CD8$^+$ T cells kill virus-infected cells early after infection. Fluorescence-activated cell sorting (FACS) dot plots showing intracellular p24 staining of HLA-B*27:05-positive U937 CD4$^+$ cells after HIV-VLP infection gated on uninfected cells and cocultured with no CD8$^+$ or KK10Gag-, KY9Pol-, orVL9Vpr-specific or mismatched CD8$^+$ T cells shown at 8 h (A) or plotted for all 5 time points as the percentages of CD4$^+$ T cells expressing p24 relative to cells without CD8$^+$ T cells added (mean values and standard errors of the means [SEM] from triplicates (B). (C and D) Gag-, Pol-, and Vpr-specific CD8$^+$ T cell killing monitored by GFP expression in virus-infected cells. FACS plots showing GFP-expressing HLA-B*27:05-positive U937 CD4$^+$ cells after HIV-VLP infection controlled by uninfected cells and cocultured with no CD8$^+$ or KK10Gag-, KY9Pol-, or VL9Vpr-specific or mismatched CD8$^+$ T cells shown at 20 h postinfection (C) and plotted for two time points as mean values and SEM of triplicates (D). (E) Data from panel B were plotted on the left *y* axis; the percentage of maximum CD8$^+$ T cell activation (CD107a/MIP1β) was plotted on the right *y* axis; data are shown for the three individual CD8$^+$ T cell lines as mean values and SEM from triplicates.

may be linked to the defective ribosomal product (DRiP) pathway (45). This pathway leads to the formation of DRiPs from the *de novo* proteins as substrates for the proteosome to improved class I presentation (46). As a consequence, the DRiP pathway will enhance presentation of epitopes from smaller viral proteins to overcome the threshold for epitope presentation as observed for the VL9Vpr epitope.

There are very limited data regarding the early events in the kinetics of antigen presentation for HIV-1 epitopes. Early antigen presentation has been previously shown for several SIV epitopes (19, 20). However, these results cannot be completely extrapolated to HIV-1 epitopes. Additionally, although various antigen presentation studies have been carried out for HIV-1 (22, 23), their readouts are not based on a single cycle of virus replication and rely on a unique target cell line. Thus, our work overcomes the limitations of previous studies by monitoring the kinetics of epitope presentation during a single cycle of HIV-1 replication and testing the consistency of our results in various cell types.

Though the early KF11Gag, KK10Gag, and KY9Pol presentation kinetics found in this study are supported by previous work (19, 20), it is still unknown which mechanisms control early presentation and immunodominance of certain epitopes over others. Certainly, the kinetics of peptide presentation do not on their own determine immunodominance. The kinetics of antigen presentation may be important in potentially having an impact on the effectiveness of certain HIV-specific CD8$^+$ T cell responses, since the earlier the recognition, the more likely it is that the cell will be killed before the release of new virions and the less likely that the CD8$^+$ T cells will be affected by Nef-mediated class I downregulation. Thus, whether the immunodominant CD8$^+$ T cell response is one that acts early or late following virus infection of target cells may be critically important in shaping the effectiveness of the anti-HIV CD8$^+$ T cell response in different individuals.

In recent years, multiple studies associated Gag-specific CD8$^+$ T cell responses with improved virus immune control (7, 16, 47). This is consistent with our findings of early presentation and killing of infected cells mediated by KF11Gag and KK10Gag protective epitopes. However, it should be pointed out that this is not the case for all Gag epitopes (21), and early presentation of certain epitopes within the small viral proteins has been previously described, in particular with examples from Nef, Rev, and Vpr epitopes being presented early as a result of being virion associated and prior to *de novo* synthesis of these proteins (18, 48–50). Therefore, these data suggest that epitope presentation does not depend

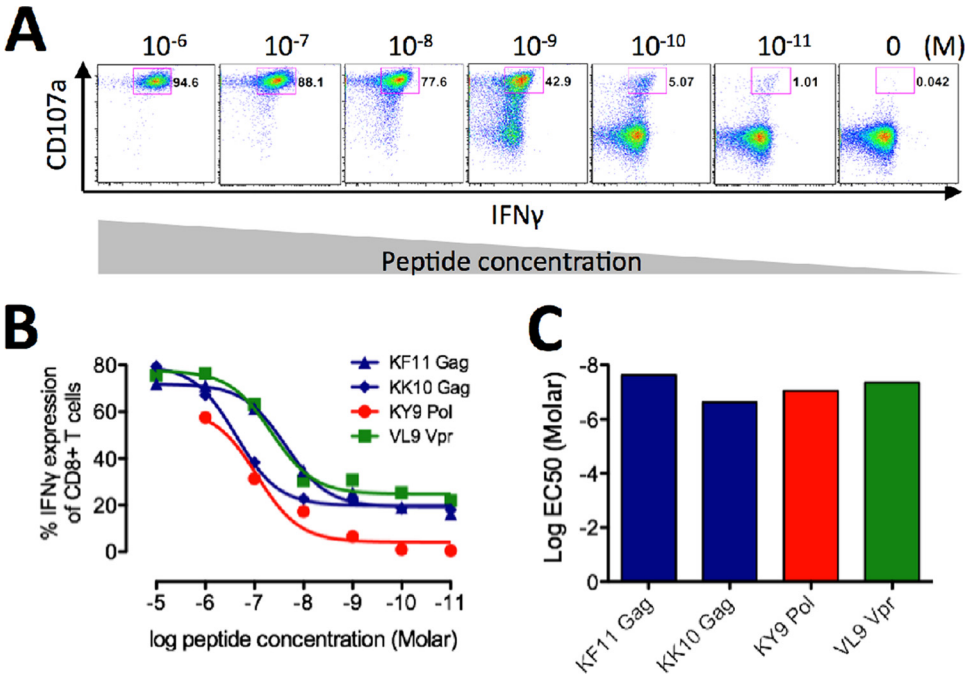

FIG 6 TcR affinities of enriched $CD8^+$ T cells. Fluorescence-activated cell sorting (FACS) plots showing CD107a- and IFN-γ-producing KY9Pol-specific $CD8^+$ T cells after peptide-titrated presentation on HLA-matched B cell line (A) with IC_{50} curves shown for KF11Gag-, KK10Gag-, KY9Pol-, and VL9Vpr-specific $CD8^+$ T cells (B) and plotted as log EC_{50} values (C).

on HIV-1 protein specificity exclusively but also on epitope properties (49) as well as other antigen-processing factors (51, 52). For example, the special feature of improved stability between dibasic N-terminal peptides for HLA-B*27:05 may result in KK10Gag and KY9Pol epitopes being more stable in the cytosol than VL9Vpr (53).

In addition, the protein-specific source from which the epitope is derived may have an important role in driving an uneven balance in antigen presentation. Epitopes derived from more-abundant viral proteins, such as Gag, which accounts for one-half of the mass in the viral particle (54), may be an initial advantage over smaller proteins to compete for class I processing machinery immediately after viral entry, further increased by posttranscriptional Gag ubiquitination (46). Early antigen presentation kinetics of important Gag epitopes KF11Gag and KK10Gag further help to explain the dominant and protective role of $CD8^+$ T cell responses against these epitopes (7–9, 25, 26, 28), in which early presentation before HLA-I downregulation (48) contributes to rapid $CD8^+$ T cell activation. As a result, early presentation of KF11Gag, KK10Gag, or KY9Pol epitopes contributes to eliminate virus-infected cells before the *de novo* production of infectious viral particles, preventing new rounds of infection and virus spread.

It may be argued that our experiments could be biased by an abnormally high number of virus-infected cells, as these experiments were performed at MOI between 0.2 and 1 depending on the cell type used, and therefore this infectious dose is expected to be of a magnitude similar to that found *in vivo* or in cell-to-cell transmission events (55). However, our study has a few limitations. First, it is important to note the limitation of using VSV-G pseudotyped virus that may differ in viral entry mechanisms from HIV-1, using receptor-mediated pH-independent cell membrane fusion, and from HIV-VLP, using a pH-dependent endocytic pathway to access the class I presentation pathway (56). However, both mechanisms of virus entrance lead to the release of intact cores to the cytosol, feeding viral antigen into the class I presentation pathway (57), and therefore similar early epitope presentations are consistently seen in HIV-1 and HIV-VLP infections. Second, our data are limited to four HIV specificities (KF11Gag, KK10Gag, KY9Pol, and VL9 Vpr) restricted by HLA- B57:01 and B27:05 and derived from polyclonal TcR clonotypes, and generalized conclusions therefore cannot necessarily be drawn from these results.

In this study, we found a decrease in total $CD8^+$ T cell activation mediated by virus-infected cells compared to that mediated by extracellular peptide-pulsed cells, which suggests that very small amounts of peptides are presented on the surface of HIV-1-infected cells. We determined that standard peptide pulse experiments use 10^3- to 10^5-higher peptide concentrations, as previously calculated (40), and likely overestimate the magnitude and functionality of total $CD8^+$ T cell responses. These results further call for a rigorous definition of $CD8^+$ T cell correlates of immune protection (58).

In conclusion, the data presented here are a proof of principle to show how key epitopes, important for HIV-1 immune control, are presented early in the virus life cycle directly from the incoming viral particles, resulting in rapid $CD8^+$ T cell activation and elimination of virus-infected cells. Based on these data, we suggest that dominant targeting of early-presented epitopes may be an important element for a rapid and initial immune control of HIV-1 infection. However, the epitopes studied here cannot necessarily be extrapolated to protein-specific properties, and further studies including additional specificities and additional HLA class

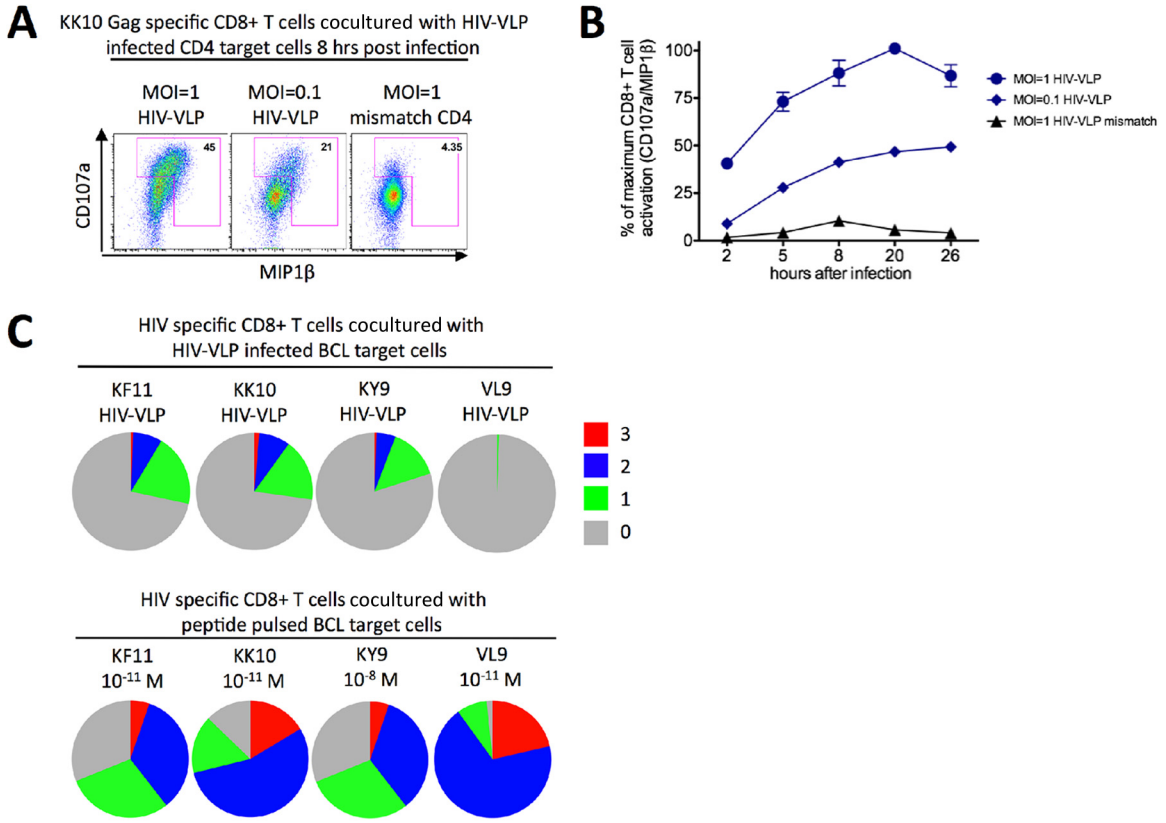

FIG 7 The magnitude of $CD8^+$ T cell activation is directly related to the dose of viral antigen. Fluorescence-activated cell sorting (FACS) plots showing CD107a/MIP1β-expressing KK10Gag- and HLA-mismatched (KF11Gag)-specific $CD8^+$-gated T cells after coculture at 8 h with U937 $CD4^+$ cells infected with of HIV-VLP at a MOI of either 1 or 0.1 (A) and plotted onto a graph for 5 time points throughout the 26 h as mean values and standard errors of the means from triplicates (B). (C) Pie charts showing the simultaneous expression of three effector molecules (IFN-γ, CD107a, and MIP1β) as 3 functions (red), 2 functions (blue), 1 function (green), or nonactivated $CD8^+$ T cells (gray) after HIV-VLP infection of B cells (top) or peptide pulsing of B cells at the peptide concentrations indicated above the pie charts (bottom) for KF11Gag-, KK10Gag-, KY9Pol-, and VL9Vpr-specific $CD8^+$ T cells.

I restriction elements are needed before general conclusions may be drawn.

ACKNOWLEDGMENTS

This work was supported by grants CP09/00279 and PI11/00249 by the ISCIII and the HIV Vaccine Catalonian Program (HIVACAT program). J.G.P. holds a Miguel Servet Contract (MS09/00279) funded by FIS-ISCIII (Spanish Government). G.J.T. holds a Wellcome Trust Senior fellowship and has funding from the Medical Research Council and the National Institutes of Health UCL/UCLH Comprehensive Biomedical Research Centre.

We thank Paul Bowness (Oxford, United Kingdom) for the HIV-1-permissive U937 cell line transfected with the HLA-B*27:05 gene. We thank study participants and C. J. Molina and E. Adland for strategic support.

We declare that we have no conflicts of interest.

REFERENCES

1. **Virgin HW, Walker BD.** 2010. Immunology and the elusive AIDS vaccine. Nature **464**:224–231.
2. **Walker BD, Burton DR.** 2008. Toward an AIDS vaccine. Science **320**: 760–764.
3. **McMichael AJ, Borrow P, Tomaras GD, Goonetilleke N, Haynes BF.** 2010. The immune response during acute HIV-1 infection: clues for vaccine development. Nat. Rev. Immunol. **10**:11–23.
4. **Kiepiela P, Leslie AJ, Honeyborne I, Ramduth D, Thobakgale C, Chetty S, Rathnavalu P, Moore C, Pfafferott KJ, Hilton L, Zimbwa P, Moore S, Allen T, Brander C, Addo MM, Altfeld M, James I, Mallal S, Bunce M, Barber LD, Szinger J, Day C, Klenerman P, Mullins J, Korber B, Coovadia HM, Walker BD, Goulder PJ.** 2004. Dominant influence of HLA-B in mediating the potential co-evolution of HIV and HLA. Nature **432**:769–775.
5. **Leslie A, Matthews PC, Listgarten J, Carlson JM, Kadie C, Ndung'u T, Brander C, Coovadia H, Walker BD, Heckerman D, Goulder PJ.** 2010. Additive contribution of HLA class I alleles in the immune control of HIV-1 infection. J. Virol. **84**:9879–9888.
6. **O'Brien SJ, Gao X, Carrington M.** 2001. HLA and AIDS: a cautionary tale. Trends Mol. Med. **7**:379–381.
7. **Kiepiela P, Ngumbela K, Thobakgale C, Ramduth D, Honeyborne I, Moodley E, Reddy S, de Pierres C, Mncube Z, Mkhwanazi N, Bishop K, van der Stok M, Nair K, Khan N, Crawford H, Payne R, Leslie A, Prado J, Prendergast A, Frater J, McCarthy N, Brander C, Learn GH, Nickle D, Rousseau C, Coovadia H, Mullins JI, Heckerman D, Walker BD, Goulder P.** 2007. CD8+ T-cell responses to different HIV proteins have discordant associations with viral load. Nat. Med. **13**:46–53.
8. **Crawford H, Lumm W, Leslie A, Schaefer M, Boeras D, Prado JG, Tang J, Farmer P, Ndung'u T, Lakhi S, Gilmour J, Goepfert P, Walker BD, Kaslow R, Mulenga J, Allen S, Goulder PJ, Hunter E.** 2009. Evolution of HLA-B*5703 HIV-1 escape mutations in HLA-B*5703-positive individuals and their transmission recipients. J. Exp. Med. **206**:909–921.
9. **Schneidewind A, Brockman MA, Yang R, Adam RI, Li B, Le Gall S, Rinaldo CR, Craggs SL, Allgaier RL, Power KA, Kuntzen T, Tung CS, LaBute MX, Mueller SM, Harrer T, McMichael AJ, Goulder PJ, Aiken C, Brander C, Kelleher AD, Allen TM.** 2007. Escape from the dominant HLA-B27-restricted cytotoxic T-lymphocyte response in Gag is associated

with a dramatic reduction in human immunodeficiency virus type 1 replication. J. Virol. **81**:12382–12393.
10. **Almeida JR, Price DA, Papagno L, Arkoub ZA, Sauce D, Bornstein E, Asher TE, Samri A, Schnuriger A, Theodorou I, Costagliola D, Rouzioux C, Agut H, Marcelin AG, Douek D, Autran B, Appay V.** 2007. Superior control of HIV-1 replication by CD8+ T cells is reflected by their avidity, polyfunctionality, and clonal turnover. J. Exp. Med. **204**:2473–2485.
11. **Betts MR, Nason MC, West SM, De Rosa SC, Migueles SA, Abraham J, Lederman MM, Benito JM, Goepfert PA, Connors M, Roederer M, Koup RA.** 2006. HIV nonprogressors preferentially maintain highly functional HIV-specific CD8+ T cells. Blood **107**:4781–4789.
12. **Duvall MG, Precopio ML, Ambrozak DA, Jaye A, McMichael AJ, Whittle HC, Roederer M, Rowland-Jones SL, Koup RA.** 2008. Polyfunctional T cell responses are a hallmark of HIV-2 infection. Eur. J. Immunol. **38**:350–363.
13. **Ferre AL, Hunt PW, Critchfield JW, Young DH, Morris MM, Garcia JC, Pollard RB, Yee HF, Jr, Martin JN, Deeks SG, Shacklett BL.** 2009. Mucosal immune responses to HIV-1 in elite controllers: a potential correlate of immune control. Blood **113**:3978–3989.
14. **Bennett MS, Ng HL, Dagarag M, Ali A, Yang OO.** 2007. Epitope-dependent avidity thresholds for cytotoxic T-lymphocyte clearance of virus-infected cells. J. Virol. **81**:4973–4980.
15. **Saez-Cirion A, Lacabaratz C, Lambotte O, Versmisse P, Urrutia A, Boufassa F, Barre-Sinoussi F, Delfraissy JF, Sinet M, Pancino G, Venet A.** 2007. HIV controllers exhibit potent CD8 T cell capacity to suppress HIV infection ex vivo and peculiar cytotoxic T lymphocyte activation phenotype. Proc. Natl. Acad. Sci. U. S. A. **104**:6776–6781.
16. **Saez-Cirion A, Sinet M, Shin SY, Urrutia A, Versmisse P, Lacabaratz C, Boufassa F, Avettand-Fenoel V, Rouzioux C, Delfraissy JF, Barre-Sinoussi F, Lambotte O, Venet A, Pancino G.** 2009. Heterogeneity in HIV suppression by CD8 T cells from HIV controllers: association with Gag-specific CD8 T cell responses. J. Immunol. **182**:7828–7837.
17. **Yang OO, Sarkis PT, Trocha A, Kalams SA, Johnson RP, Walker BD.** 2003. Impacts of avidity and specificity on the antiviral efficiency of HIV-1-specific CTL. J. Immunol. **171**:3718–3724.
18. **Sacha JB, Buechler MB, Newman LP, Reed J, Wallace LT, Loffredo JT, Wilson NA, Watkins DI.** 2010. Simian immunodeficiency virus-specific CD8+ T cells recognize Vpr- and Rev-derived epitopes early after infection. J. Virol. **84**:10907–10912.
19. **Sacha JB, Chung C, Rakasz EG, Spencer SP, Jonas AK, Bean AT, Lee W, Burwitz BJ, Stephany JJ, Loffredo JT, Allison DB, Adnan S, Hoji A, Wilson NA, Friedrich TC, Lifson JD, Yang OO, Watkins DI.** 2007. Gag-specific CD8+ T lymphocytes recognize infected cells before AIDS-virus integration and viral protein expression. J. Immunol. **178**:2746–2754.
20. **Sacha JB, Chung C, Reed J, Jonas AK, Bean AT, Spencer SP, Lee W, Vojnov L, Rudersdorf R, Friedrich TC, Wilson NA, Lifson JD, Watkins DI.** 2007. Pol-specific CD8+ T cells recognize simian immunodeficiency virus-infected cells prior to Nef-mediated major histocompatibility complex class I downregulation. J. Virol. **81**:11703–11712.
21. **Sacha JB, Reynolds MR, Buechler MB, Chung C, Jonas AK, Wallace LT, Weiler AM, Lee W, Piaskowski SM, Soma T, Friedrich TC, Wilson NA, Watkins DI.** 2008. Differential antigen presentation kinetics of CD8+ T-cell epitopes derived from the same viral protein. J. Virol. **82**:9293–9298.
22. **Ali A, Lubong R, Ng H, Brooks DG, Zack JA, Yang OO.** 2004. Impacts of epitope expression kinetics and class I downregulation on the antiviral activity of human immunodeficiency virus type 1-specific cytotoxic T lymphocytes. J. Virol. **78**:561–567.
23. **van Baalen CA, Guillon C, van Baalen M, Verschuren EJ, Boers PH, Osterhaus AD, Gruters RA.** 2002. Impact of antigen expression kinetics on the effectiveness of HIV-specific cytotoxic T lymphocytes. Eur. J. Immunol. **32**:2644–2652.
24. **Payne RP, Kloverpris H, Sacha JB, Brumme Z, Brumme C, Buus S, Sims S, Hickling S, Riddell L, Chen F, Luzzi G, Edwards A, Phillips R, Prado JG, Goulder PJ.** 2010. Efficacious early antiviral activity of HIV Gag- and Pol-specific HLA-B*2705-restricted CD8+ T cells. J. Virol. **84**:10543–10557.
25. **Crawford H, Prado JG, Leslie A, Hue S, Honeyborne I, Reddy S, van der Stok M, Mncube Z, Brander C, Rousseau C, Mullins JI, Kaslow R, Goepfert P, Allen S, Hunter E, Mulenga J, Kiepiela P, Walker BD, Goulder PJ.** 2007. Compensatory mutation partially restores fitness and delays reversion of escape mutation within the immunodominant HLA-B*5703-restricted Gag epitope in chronic human immunodeficiency virus type 1 infection. J. Virol. **81**:8346–8351.
26. **Feeney ME, Tang Y, Roosevelt KA, Leslie AJ, McIntosh K, Karthas N, Walker BD, Goulder PJ.** 2004. Immune escape precedes breakthrough human immunodeficiency virus type 1 viremia and broadening of the cytotoxic T-lymphocyte response in an HLA-B27-positive long-term-nonprogressing child. J. Virol. **78**:8927–8930.
27. **Goulder PJ, Brander C, Tang Y, Tremblay C, Colbert RA, Addo MM, Rosenberg ES, Nguyen T, Allen R, Trocha A, Altfeld M, He S, Bunce M, Funkhouser R, Pelton SI, Burchett SK, McIntosh K, Korber BT, Walker BD.** 2001. Evolution and transmission of stable CTL escape mutations in HIV infection. Nature **412**:334–338.
28. **Goulder PJ, Phillips RE, Colbert RA, McAdam S, Ogg G, Nowak MA, Giangrande P, Luzzi G, Morgan B, Edwards A, McMichael AJ, Rowland-Jones S.** 1997. Late escape from an immunodominant cytotoxic T-lymphocyte response associated with progression to AIDS. Nat. Med. **3**:212–217.
29. **Shimizu Y, DeMars R.** 1989. Production of human cells expressing individual transferred HLA-A,-B,-C genes using an HLA-A,-B,-C null human cell line. J. Immunol. **142**:3320–3328.
30. **Prado JG, Honeyborne I, Brierley I, Puertas MC, Martinez-Picado J, Goulder PJ.** 2009. Functional consequences of human immunodeficiency virus escape from an HLA-B*13-restricted CD8+ T-cell epitope in p1 Gag protein. J. Virol. **83**:1018–1025.
31. **Weber J, Weberova J, Carobene M, Mirza M, Martinez-Picado J, Kazanjian P, Quinones-Mateu ME.** 2006. Use of a novel assay based on intact recombinant viruses expressing green (EGFP) or red (DsRed2) fluorescent proteins to examine the contribution of pol and env genes to overall HIV-1 replicative fitness. J. Virol. Methods **136**:102–117.
32. **Zufferey R, Nagy D, Mandel RJ, Naldini L, Trono D.** 1997. Multiply attenuated lentiviral vector achieves efficient gene delivery in vivo. Nat. Biotechnol. **15**:871–875.
33. **Bainbridge JW, Stephens C, Parsley K, Demaison C, Halfyard A, Thrasher AJ, Ali RR.** 2001. In vivo gene transfer to the mouse eye using an HIV-based lentiviral vector; efficient long-term transduction of corneal endothelium and retinal pigment epithelium. Gene Ther. **8**:1665–1668.
34. **Naldini L, Blomer U, Gallay P, Ory D, Mulligan R, Gage FH, Verma IM, Trono D.** 1996. In vivo gene delivery and stable transduction of nondividing cells by a lentiviral vector. Science **272**:263–267.
35. **Besnier C, Takeuchi Y, Towers G.** 2002. Restriction of lentivirus in monkeys. Proc. Natl. Acad. Sci. U. S. A. **99**:11920–11925.
36. **Sacha JB, Watkins DI.** 2010. Synchronous infection of SIV and HIV in vitro for virology, immunology and vaccine-related studies. Nat. Protoc. **5**:239–246.
37. **Freel SA, Lamoreaux L, Chattopadhyay PK, Saunders K, Zarkowsky D, Overman RG, Ochsenbauer C, Edmonds TG, Kappes JC, Cunningham CK, Denny TN, Weinhold KJ, Ferrari G, Haynes BF, Koup RA, Graham BS, Roederer M, Tomaras GD.** 2010. Phenotypic and functional profile of HIV-inhibitory CD8 T cells elicited by natural infection and heterologous prime/boost vaccination. J. Virol. **84**:4998–5006.
38. **Addo MM, Yu XG, Rathod A, Cohen D, Eldridge RL, Strick D, Johnston MN, Corcoran C, Wurcel AG, Fitzpatrick CA, Feeney ME, Rodriguez WR, Basgoz N, Draenert R, Stone DR, Brander C, Goulder PJ, Rosenberg ES, Altfeld M, Walker BD.** 2003. Comprehensive epitope analysis of human immunodeficiency virus type 1 (HIV-1)-specific T-cell responses directed against the entire expressed HIV-1 genome demonstrate broadly directed responses, but no correlation to viral load. J. Virol. **77**:2081–2092.
39. **Draenert R, Altfeld M, Brander C, Basgoz N, Corcoran C, Wurcel AG, Stone DR, Kalams SA, Trocha A, Addo MM, Goulder PJ, Walker BD.** 2003. Comparison of overlapping peptide sets for detection of antiviral CD8 and CD4 T cell responses. J. Immunol. Methods **275**:19–29.
40. **Varela-Rohena A, Molloy PE, Dunn SM, Li Y, Suhoski MM, Carroll RG, Milicic A, Mahon T, Sutton DH, Laugel B, Moysey R, Cameron BJ, Vuidepot A, Purbhoo MA, Cole DK, Phillips RE, June CH, Jakobsen BK, Sewell AK, Riley JL.** 2008. Control of HIV-1 immune escape by CD8 T cells expressing enhanced T-cell receptor. Nat. Med. **14**:1390–1395.
41. **Ranki A, Lagerstedt A, Ovod V, Aavik E, Krohn KJ.** 1994. Expression kinetics and subcellular localization of HIV-1 regulatory proteins Nef, Tat and Rev in acutely and chronically infected lymphoid cell lines. Arch. Virol. **139**:365–378.
42. **Kafri T, Morgan D, Krahl T, Sarvetnick N, Sherman L, Verma I.** 1998.

Cellular immune response to adenoviral vector infected cells does not require de novo viral gene expression: implications for gene therapy. Proc. Natl. Acad. Sci. U. S. A. **95**:11377–11382.
43. **Riddell SR, Rabin M, Geballe AP, Britt WJ, Greenberg PD.** 1991. Class I MHC-restricted cytotoxic T lymphocyte recognition of cells infected with human cytomegalovirus does not require endogenous viral gene expression. J. Immunol. **146**:2795–2804.
44. **Yewdell JW, Bennink JR, Hosaka Y.** 1988. Cells process exogenous proteins for recognition by cytotoxic T lymphocytes. Science **239**:637–640.
45. **Yewdell JW, Nicchitta CV.** 2006. The DRiP hypothesis decennial: support, controversy, refinement and extension. Trends Immunol. **27**:368–373.
46. **Hahn S, Setz C, Wild J, Schubert U.** 2011. The PTAP sequence within the p6 domain of human immunodeficiency virus type 1 Gag regulates its ubiquitination and MHC class I antigen presentation. J. Immunol. **186**:5706–5718.
47. **Honeyborne I, Prendergast A, Pereyra F, Leslie A, Crawford H, Payne R, Reddy S, Bishop K, Moodley E, Nair K, van der Stok M, McCarthy N, Rousseau CM, Addo M, Mullins JI, Brander C, Kiepiela P, Walker BD, Goulder PJ.** 2007. Control of human immunodeficiency virus type 1 is associated with HLA-B*13 and targeting of multiple gag-specific CD8+ T-cell epitopes. J. Virol. **81**:3667–3672.
48. **Chen DY, Balamurugan A, Ng HL, Cumberland WG, Yang OO.** 2012. Epitope targeting and viral inoculum are determinants of Nef-mediated immune evasion of HIV-1 from cytotoxic T lymphocytes. Blood **120**:100–111.
49. **Chen DY, Balamurugan A, Ng HL, Yang OO.** 2011. Antiviral activity of human immunodeficiency virus type 1 Gag-specific cytotoxic T lymphocyte targeting is not necessarily intrinsically superior to envelope targeting. J. Virol. **85**:2474–2478.
50. **Sacha JB, Giraldo-Vela JP, Buechler MB, Martins MA, Maness NJ, Chung C, Wallace LT, Leon EJ, Friedrich TC, Wilson NA, Hiraoka A, Watkins DI.** 2009. Gag- and Nef-specific CD4+ T cells recognize and inhibit SIV replication in infected macrophages early after infection. Proc. Natl. Acad. Sci. U. S. A. **106**:9791–9796.
51. **Yewdell JW, Haeryfar SM.** 2005. Understanding presentation of viral antigens to CD8+ T cells in vivo: the key to rational vaccine design. Annu. Rev. Immunol. **23**:651–682.
52. **Yewdell JW, Reits E, Neefjes J.** 2003. Making sense of mass destruction: quantitating MHC class I antigen presentation. Nat. Rev. Immunol. **3**:952–961.
53. **Herberts CA, Neijssen JJ, de Haan J, Janssen L, Drijfhout JW, Reits EA, Neefjes JJ.** 2006. Cutting edge: HLA-B27 acquires many N-terminal dibasic peptides: coupling cytosolic peptide stability to antigen presentation. J. Immunol. **176**:2697–2701.
54. **Jacks T, Power MD, Masiarz FR, Luciw PA, Barr PJ, Varmus HE.** 1988. Characterization of ribosomal frameshifting in HIV-1 gag-pol expression. Nature **331**:280–283.
55. **Jolly C, Kashefi K, Hollinshead M, Sattentau QJ.** 2004. HIV-1 cell to cell transfer across an Env-induced, actin-dependent synapse. J. Exp. Med. **199**:283–293.
56. **Buseyne F, Le Gall S, Boccaccio C, Abastado JP, Lifson JD, Arthur LO, Riviere Y, Heard JM, Schwartz O.** 2001. MHC-I-restricted presentation of HIV-1 virion antigens without viral replication. Nat. Med. **7**:344–349.
57. **Schaller T, Ocwieja KE, Rasaiyaah J, Price AJ, Brady TL, Roth SL, Hue S, Fletcher AJ, Lee K, KewalRamani VN, Noursadeghi M, Jenner RG, James LC, Bushman FD, Towers GJ.** 2011. HIV-1 capsid-cyclophilin interactions determine nuclear import pathway, integration targeting and replication efficiency. PLoS Pathog. **7**:e1002439. doi:10.1371/journal.ppat.1002439.
58. **Prado JG, Carrillo J, Blanco-Heredia J, Brander C.** 2011. Immune correlates of HIV control. Curr. Med. Chem. **18**:3963–3970.